Micromachining Characterization of Ultrathin Ni-membranes

ICOMM 2014 No. 69

Vijay Mahawar, Kundan K. Singh, Ramesh K. Singh

Department of Mechanical Engineering, Indian Institute of Technology Bombay, Mumbai, Powai-400076, India

Abstract

Thin membranes of different materials find extensive use in fabrication of Micro Electro Mechanical Systems (MEMS) devices. Machined membranes are used as heat sinks by fabricating micro channels for high heat transfer rates in micro heat exchanger and as membrane stacks of Proton Exchange Membrane fuel cells. These membranes can also be used as masks for lithography for creating features on silicon wafers for semiconductor industry. Due to low flexural rigidity of the ultra-thin membranes, fixturing of membranes poses additional challenges. The plastic deformation induced during machining and the burr formation/tearing needs to be minimized for improving the geometrical accuracy of the machined feature. The cutting forces in membrane machining are very small in magnitude and an accurate model for the prediction of these forces needs to be developed and validated. The current study focuses on micromilling of ultrathin membranes. A parametric study of micromilling parameters has been conducted to characterize the geometrical accuracy of machined micro slots on two workpieces, ultra-thin (20 μm) pure Ni membranes and relatively thick (200 μm) pure Ni workpiece. A mechanistic model for cutting forces has been developed for thin membranes to predict forces involved and has been validated with the experimental data. Scanning electron microscopy (SEM), white light interferometer (WLI) and optical microscope were used for characterization of dimensional accuracy of micro slots geometry in terms of their width. The minimum geometrical accuracies error obtained were 50% and 19% for 100μm and 400μm tools respectively for 20μm thin Ni membrane and 7% for 200μm thick Ni workpiece using 400μm tool. Cutting forces are measured using a three directional Kristler dynamometer (Minidyne 9256 C2) for both the thickness of workpieces. The maximum resultant cutting forces of X and Y directions were 1.3 N at the feed rate of 10um/flute and 60000 RPM for 20μm thin Ni membrane which is quite low as compared to thick materials.

Keywords: Thin membranes, flexural rigidity, overall slot width, cutting coefficients, low and high speed micromilling, scanning electron microscopy, white light interferometer.

1. Introduction

Membranes are emerging as an important aspect of micromachining components ranging from micro heat exchanger to electronic circuits in various MEMS devices. Production of these thin membrane structures are suitable for micro-electro-mechanical systems or micro-electronic devices. Membranes of different heat conductive materials such as silver, copper, nickel etc. are used as heat sinks in micro heat exchangers. Membranes have very low flexural rigidity because their thickness is very low as compared to their length and breadth. While machining on a membrane, even a small variation in depth of cut of the tool can affect the part dimensions significantly. Therefore, machining processes which do not involve mechanical forces while machining are extensively used for machining membrane for the desired patterns for the fabrication of micro heat exchanger, fuel cells etc. Machined micro patterns on thin membranes are essential part of any Micro-Electro Mechanical Systems (MEMS). A variety of micromachining processes are available for machining micro patterns on thin membranes. In various micro electro mechanical systems polymer microfluidic devices are being used extensively. A variety of manufacturing processes to produce the thin embossing mold for fabrication of these micro fluidic devices have been proposed in the literature such as the electroplating process [1] and nickel UV–LiGA [2], chemical etching etc. These processes have successfully fabricated the mold with thicknesses down to 50-100 μm. However, these processes consist of multiple stages and operations on the workpiece and are very expensive. High-precision micromilling requires less steps compared to LiGA [3,4], and consumes less time [5].

There are several challenges in machining of thin membranes through micromilling, such as induced stresses and deformations, fixturing challenges because of low flexural rigidity, and interaction of the membrane with the milling cutter. The deformation and stress induced by the machining process may be significant and lead to tearing of membranes during the micromilling process. The challenge of how to fixture the membrane to withstand machining induced loads, while itself not contributing to residual stress and deformation, needs to be addressed. In addition, the cutting mechanism and plastic deformation of the membranes may also be affected by the interaction of end-mill cutter and membrane [6]. The factors in micromilling which affect cutting mechanisms in micro scale machining, such as minimum chip thickness criterion, chip formation, cutting edge radius effects and influence of workpiece

micro structure grain size [7] are extensively studied for thick materials by lot of researchers in details where the flexural rigidity of the work piece is high. The cutting mechanism and cutting forces dynamics are significantly affected by these factors when operating in different parametric machining zones. These factors are important for the process quality point of view and lead to the instability of process with dimensional inaccuracies. For reducing the effects of these factors, an optimum zone of machining parameters has to be determined.

Micromilling is an effective machining process which can be used to create 3D free-form micro-scale features in a wide range of engineering materials. Micro end milling can be considered as a miniaturized version of the conventional end milling process [8]. Chip formation in micromilling is influenced by the edge radius (generally 2µm -4µm) of the cutter [9]. Ploughing of the workpiece takes place instead of cutting when the uncut chip thickness is less than or comparable to the cutting edge radius of the tool [10]. The forces involved in micro end milling are very small as compared to conventional end milling and the cutting forces during machining of ultrathin membranes are even smaller. The micromilling operation is susceptible to tool wear and catastrophic tool failure and noises in cutting force measurement. Thus, the modeling and understanding of microcutting forces are important to predict the dynamics of the process, machined part quality and dimensional accuracies.

While investigations in microcutting of thick workpieces have been widely reported, those in microcutting thin membranes (of the order of few µm) are rare. The current study focuses on the effect of the process parameters in micromachining of ultrathin Ni membrane. The aim is to see that whether the membranes when machined through the conventional micromilling tools behave similar to thick materials or not. This paper is focused on studying the effect of micromachining process parameters on 20 µm thin pure Ni membranes and relatively thick 200µm Ni workpiece. A mechanistic model for cutting forces prediction has been developed for ultra-thin membranes and cutting mechanism analysis has been done in terms of dimensional accuracies and burr formation mechanism.

2. Experimental Work

Fig.1 shows the flow diagram of the current work. Experimental characterization of micro slot widths at conventional micromilling speed (20000 rpm) and high speed micromilling process (100000 rpm) have been performed to study the dimensional accuracy analysis and cutting mechanism for 20µm thin pure Ni membrane and 200µm thick Ni workpiece by the effect of process parameters. A mechanistic model of cutting forces has been developed for thin membranes.

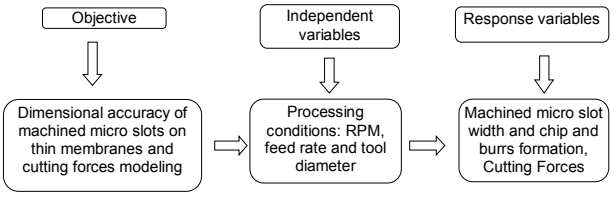

Fig.1. Flow diagram of work

2.1. Experimental Details

Parametric experiments were conducted for determining the effect of the process parameters on the geometrical accuracy of machined slots and chip formation mechanism at conventional and high rotational speeds. Preliminary experiments were conducted to determine the approximate limiting values of the process parameters. Table 1 lists the process parameters which are expected to affect the dimensional accuracies and chip formation mechanism. Table 2 lists the large variation of feed rates at 6000 RPM for identifying the ploughing and shearing dominant zones for modeling the cutting forces.

Table1. Set of the process parameters used in the experiments for 20µm thick Ni membrane for geometric characterization

Sr. No.	Spindle Speed (RPM)	Feed(µm/flute)					Tool Diameter (D) (µm)		No. of Flutes
1	20000	0.1	1	2	3	4	100	400	2
2	60000	0.1	1	2	3	4	100	400	2
3	100000	0.1	1	2	3	4	100	400	2

Table2. Set of the process parameters for developing cutting force mechanistic model

RPM	Feed (µm/flute)							
60000	0.1	0.4	0.7	1	1.3	1.6	1.9	2.1
	2.4	2.7	3	3.3	3.6	3.9	4.1	4.4
	5	5.5	6	6.5	7	7.5	8	8.5
	9	9.5	10					
Tool Diameter (µm) - 300								
No. of flutes - 2								

A parametric study has been performed varying each parameter while keeping other parameters constant. Three levels of tool rotation speed (RPM), five levels of feed rate (µm/rev/flute) and two levels of tool diameter with same number of flutes (two) have been used in the experiments. For force prediction, simulation and validation, a large range of feed/rev/flute (0.1µm-10µm) has been used The dimensional accuracy of the machined micro slot width characterization and chip formation mechanism has been conducted via scanning electron microscopy (SEM) along with white light interferometry (WYKO NT 9100®). The cutting forces in feed (F_x) and transverse (F_y) direction have been measured.

2.2. Experimental Setup and Procedure

Experimental setup is shown in Fig. 2. The machining operations were performed on a high speed micromachining center designed and developed in the Machine Tools Laboratory at IIT Bombay. The maximum spindle speed of the micromilling machining is 140,000 rpm IBAG spindle. The Z-stage is actuated by a pneumatically counter balanced linear motor and has a positioning resolution of 5 nm. The XY stacked stages are driven by precision ball screw and have a positioning resolution of 0.5µm and an accuracy of ±0.7µm.The maximum translation speed of the stages is 100 mm/s. The micro-machine is capable of creating nano-scale3D free-form

features. Uncoated tungsten carbide (WC) end-milling cutters (two flutes) were used in this study to machine the micro slots on the 20 μm thick Ni membrane with the depth of cut equal to the thickness of the membrane which means through micro slots have been machined on the membrane and a 200μm thick Ni workpiece with same depth of cut. The cutting forces are measured using a three directional Kistler dynamometer (Minidyne 9256 C2) connected to a data acquisition (National Instruments DAQ) system.

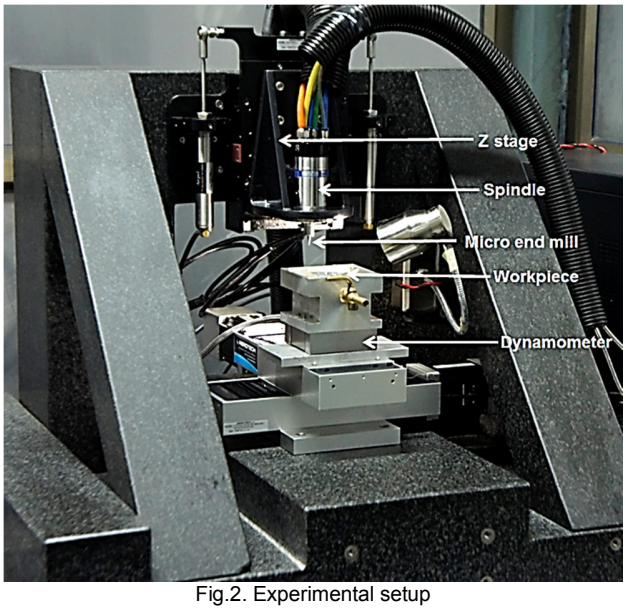

Fig.2. Experimental setup

2.3 Fixture Design

Machining of nickel membrane with fixture design is shown in Fig. 3. For the current study of machining nickel membrane, a fixture is designed. Two aluminum thick rectangular plates are used for sandwiching the membrane between them. Both the aluminum plates after extracting from the aluminum slab were polished on METAPOL-160 metal polishing machine to make them smooth and flat. A rectangular slot is made on the upper plate of aluminum through milling for providing a slot for machining on the sandwiched membrane as shown in Fig. 3.

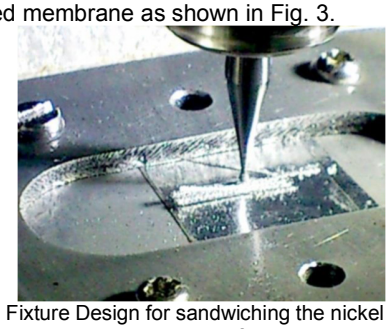
Fig.3. Fixture Design for sandwiching the nickel membranes by two aluminum flat plates

The plates then are machined on the same micromilling center where the membrane machining experiment to be performed in order to make them true with reference to the Z axis of the micromilling center. The purpose of milling of the plates on the same micromilling center is to make them flat with reference to the Z axis because even small depth of cut variation due to the plate uneven surface can cause the significant dimensional errors of the machined patterns on the membranes and tearing of membrane can be possible in such situations.

3. Mechanistic Model for Cutting Forces

A typical flat end milling cutter with two and four flutes is shown in Fig. 4. These multiple cutting edges are usually made helical to reduce the impact during the entry into the work piece.

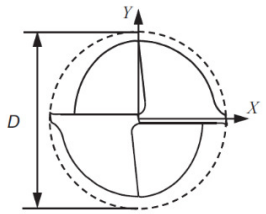

Fig .4 Geometry of helical micro end milling cutter

Fig.5 shows the Cartesian coordinate system which has been defined to denote the various cutting forces involved during the process. The centre of the coordinate system is located at the centre of the cutter. The X axis is along the feed direction with respect to the workpiece, Y axis is transverse to the feed direction and Z axis is along the cutter axis. It is a usual practice to divide the cutter into number of smaller elemental slices along the axis of the cutter. Each element is then considered as oblique cutting edge with an inclination angle to the helix angle of the cutter .The three incremental force components, namely tangential (dF_{tj}), radial (dF_{rj}) and axial (dF_{aj}) acting on a differential element (dz) of jth flute [13] can be formulated as:

$$dFtj(\theta) = [Ktc * tcj(\theta) + Kte]dz \quad (1)$$
$$dFrj(\theta) = [Krc * tcj(\theta) + Kre]dz \quad (2)$$
$$dFaj(\theta) = [Kac * tcj(\theta) + Kae]dz \quad (3)$$

where K_{tc}, K_{rc} *and* K_{ac} are the cutting force coefficients in tangential, radial and axial directions, respectively, and K_{te}, K_{re} *and* K_{ae} are the corresponding edge force coefficients. The geometry of chip formation in milling is shown in Fig 5.

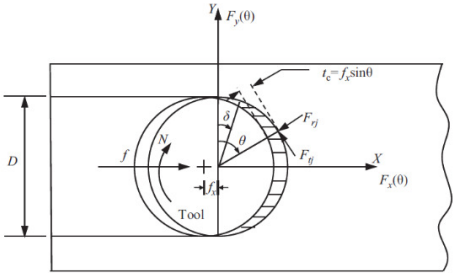

Fig. 5 Cutting mechanism in milling process [13]

In milling the instantaneous uncut chip thickness *(t_c)* varies periodically as a function of time-varying angle θ which is the tool rotation or immersion angle measured clockwise from the positive Y axis to the reference flute j. For finding

the cutting coefficients and edge coefficients, a parametric study has been done. These coefficients are unique for a given tool-work piece combinations. A number of slot milling experiments have been performed for thin nickel membrane (20 μm thin) and thick Ni workpiece (200 μm thick) with 300 μm tungsten carbide two flute end mill cutter pair. A large variation of feed (0.1 -10 μm/tooth) has been taken to first identify the ploughing and cutting dominant zone because of minimum cutting edge radius phenomenon in micro milling. The forces data (F_x, F_y and F_z) was experimentally measured for a number of feeds for identifying the cutting edge radius and the shearing dominant zone. These feed (F_x), transvers (F_y) and axial (F_z) experimental forces are then converted to tangential, radial and axial forces respectively for the determination of cutting and edge coefficients. A linear curve was fit between the RMS (root mean square) magnitude of forces and feed by minimizing the mean square error.

4. Results and Discussions

The mechanistic force model has been developed for predicting the cutting forces for thin Ni workpiece with a tungsten carbide tool. The cutting forces are then simulated and compared with the experimental forces. Cutting mechanism and burr formation in ultrathin Ni membrane and thick Ni workpiece has also been investigated and geometrical accuracy analysis has been performed as a function of the process parameters.

4.1. Mechanistic cutting force model based comparison between thick and thin pieces

A number of slot milling operations have been performed for different feeds (0.1-10um/tooth) at 60000 RPM to identify the shearing dominant zone. An end mill cutter of 300 μm diameter and 2 flutes have been used for developing the model. When the uncut chip thickness is bigger than the cutting edge radius, shearing occurs and the material starts to cut in conventional manner. This results in a substantial increase in the cutting forces. Fig. 6 and 7 show the three regions of operations (ploughing dominant, transition and shearing dominant region) for 20μm workpiece and 200 μm thick workpiece, respectively.

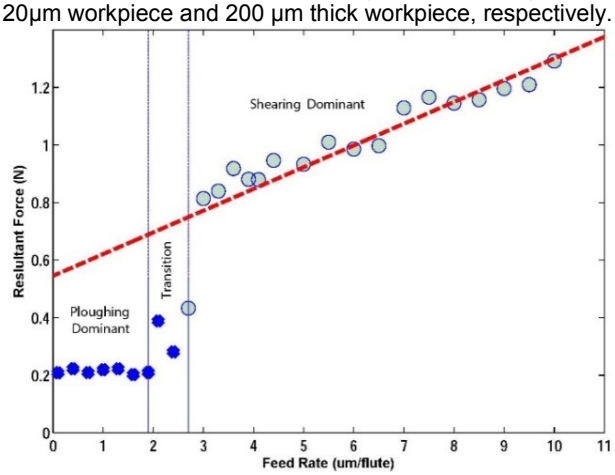

Fig. 6 Micromilling resultant forces vs. feed with depth of cut of 20 μm for 20 μm thick workpiece (300μm end mill cutter)

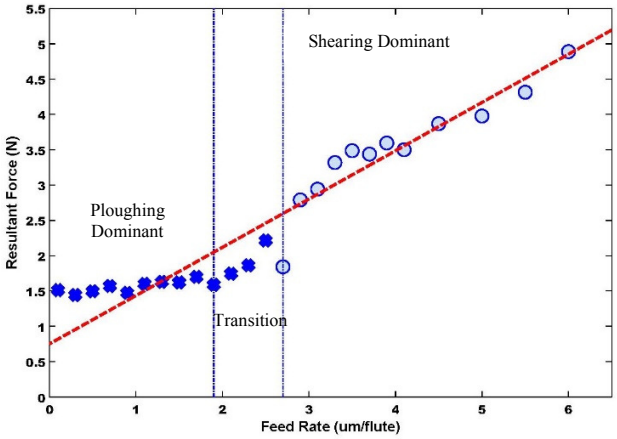

Fig. 7 Micromilling resultant forces vs. feed with depth of cut of 20 μm for 200 μm thick workpiece (300μm end mill cutter)

The resultant RMS forces increase drastically from 0.2 to 0.8 N for the thin membrane as the uncut chip thickness exceeds the critical chip thickness of ~2.7 μm (see Fig. 6). This demonstrates the minimum chip thickness phenomenon in micro milling very clearly. It is seen that the maximum resultant RMS force is not very high ~1.3 N for thin membrane as opposed to ~5 N for thick work piece as shown in Fig. 7. This difference could be attributed to through cutting in case of thin membranes which reduces the axial forces significantly and the lower flexural rigidity of the thin membrane. However, the cutting mechanism and the minimum chip thickness phenomenon follows similar trend for both thin and thick workpieces. The cutting forces for thick workpiece are significantly higher than that of the thin workpiece which could potentially lead to increased tool wear and process instability.

Fig. 8 shows the forces generated in X (Fig.(a)) and Y (Fig.8(b)) directions during machining of both 20μm and 200μm workpieces. It can be seen that the magnitude of the forces for thick workpiece are around 2-3 times higher as that of thin workpiece which can influence the process as mentioned previously. This difference in the cutting forces can affect the cutting mechanism and burr formation while machining a workpiece of different thickness.

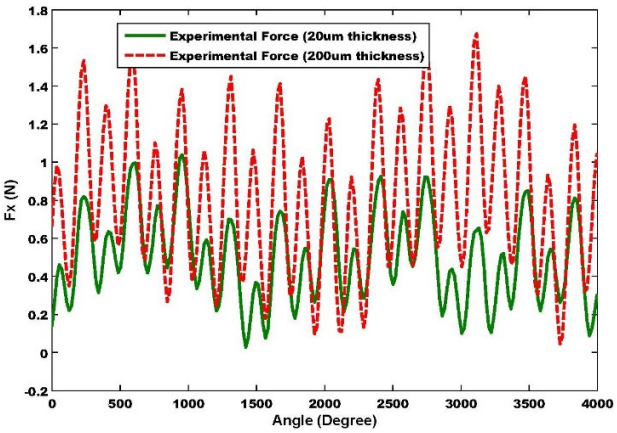

(a)

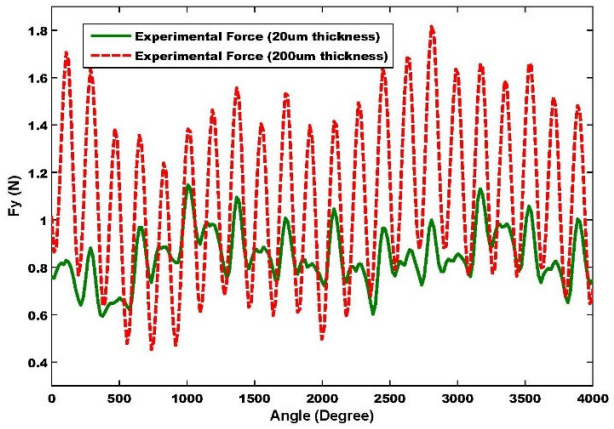

(b)

Fig. 8 Comparison of the cutting forces for different thickness of the workpiec (a) 20um thick (b) 200um thick at feed of 4.5 um/flute

Once the shearing region is determined, the cutting and edge coefficient can easily be found by a linear fit curve in shearing dominant region. The radial and tangential forces are computed. A linear curve was fit for both tangential and radial experimental forces using the RMS values of the corresponding forces at different feeds. Table 3 shows the values of cutting and edge coefficients determined experimentally.

Table. 3 Cutting constants for the shearing dominant regions for 20µm thin Ni membrane and 300 um 2 flutes tungsten carbide tool

Ktc(N/mm^2)	Krc(N/mm^2)	Kte(N/mm)	Kre(N/mm)
4000	3550	12	15

Fig. 9 shows the plots of experimental and theoretical forces obtained using identified coefficient for feed/flute of 5 µm for 20µm thin Ni membrane using 300µm 2 flute end mill cutter. The model can predict the pattern and dynamics of the experimental cutting forces as a function of cutter rotation angle. The simulated forces follows the same pattern as of experimental forces with a overshoot of 20% in amplitude at some specific cutter rotation angles but the experimental forces are confined within predicted values for most of the time. The experimental forces are in reasonably good agreement.

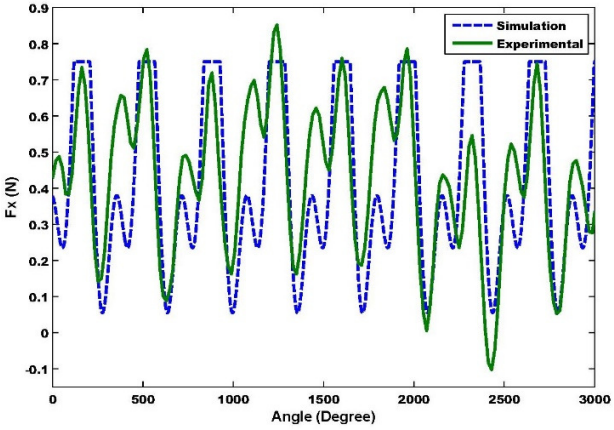

(a)

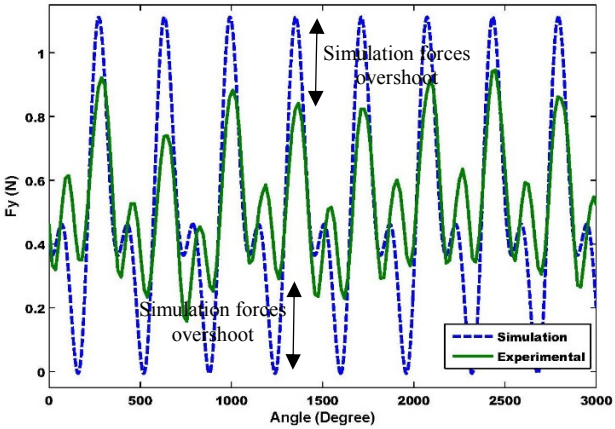

(b)

Fig. 9 Comparison of simulated and experimental forces in Feed (Fx) and Transverse (Fy) at feed of 5 µm/flute for 20µm thin Ni membrane using 300µm 2flute end mill cutter

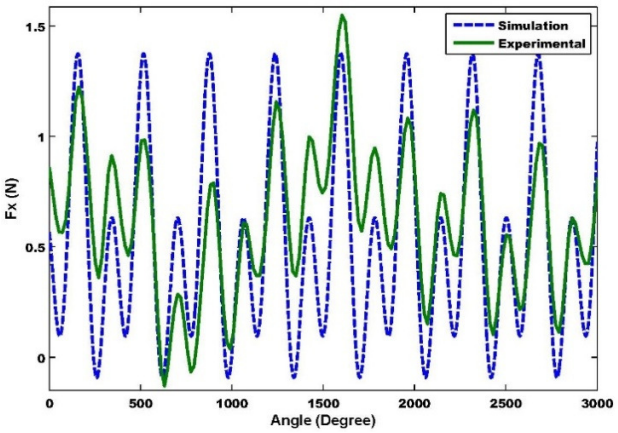

(a)

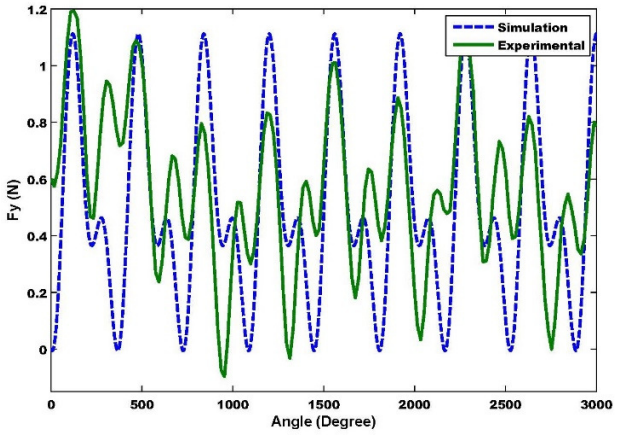

(b)

Fig. 10 Comparison of simulated and experimental forces in Feed (Fx) and Transverse (Fy) at feed of 9.5um/flute for 20µm thin Ni membrane using 300µm 2flute end mill cutter

Fig. 10 show the experimental and theoretical forces obtained using identified coefficient for feed for relatively larger feed of 9.5µm. It can be observed that the predicted forces yield conservative results and envelop the

experimental forces albeit with some overshoot and minor phase difference. The magnitude of the increase in forces is captured accurately via this model.

4.2. Burr formation and cutting mechanism

Figs. 11 and 12 show SEM images of machined micro slots on 20μm thick nickel membrane with a100μm 2-flute end mill cutter having a cutting edge radius of around 3μm both at conventional (20,000 rpm) and high (100,000) spindle rotational speeds.

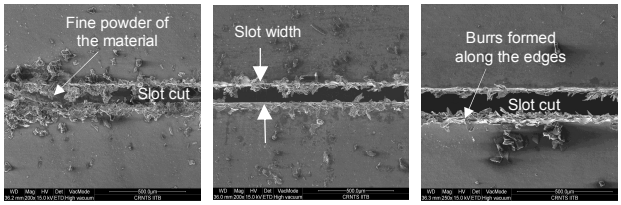

(a) (b) (c)

Fig.11. SEM images of machined micro slots at low speed milling RPM=20000 for different feed rates: (a) 0.1 μm/tooth/rev; (b) 2 μm/tooth/rev; (c) 4 μm/tooth/revfor 100μm tool diameter

Fig.11 (a) shows the machined micro slots for very low feed in low speed milling (20000 rpm). Because of very low feed rate of 0.1μm/tooth/rev instead of cutting of membrane, ploughing occurs where the chip load or uncut chip thickness is much lower than cutting edge radius (3μm). In ploughing situation, the metal is compressed by the cutting tool and recovers back, as opposed to being sheared by a sharp cutting edge to form a chip as studied by various researches in terms of minimum chip thickness effects and cutting edge radius effects [7]. Ploughing of the membrane because of low feeds results in the formation of fine powder of the material around and within the machined slots instead of chip formation. Because of the compression of the membrane rather than shearing, the process becomes highly unstable as little-to-no cutting occurs at such low chip load and the cutter just ploughs through the workpiece. Fig.11 (c) shows the machined micro slots at high chip load in low speed milling. Since, the chip load increases comparable to the cutting edge radius, the chip formation proceeds in the conventional manner with burrs formation at the edges of the machined micro slots.

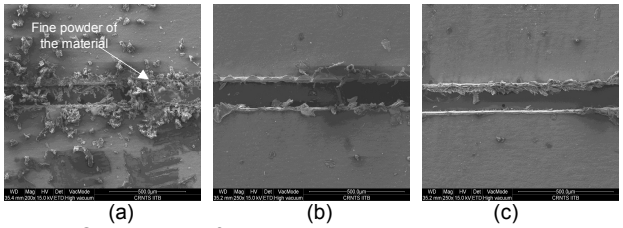

(a) (b) (c)

Fig.12. SEM images of machined micro slots at high speed milling RPM=100000 for different feed rates: (a) 0.1 μm/tooth/rev; (b) 2 μm/tooth/rev; (c) 4 μm/tooth/rev for 100μm tool diameter

Fig. 12(a) shows the machined micro slots for low chip load at 100,000 rpm. Since, the chip load is much lower than the cutting edge radius of the tool, so the tool ploughs though the membranes without forming any chips. A fine powder of the workpiece material is deposited around the slot. However with an increase in feed/tooth at higher rotational speed, the process becomes progressively more stable with significant reduction in dimensional inaccuracies of the micro machined feature. For high chip loads as shown in Fig.12 (c), cutting occurs and chips start to form effectively and the burr formation is lower in high speed cutting as compared to low speed milling Fig.11 (c).

Figs. 13 and 14 show scanning electron micrographs of machined micro slots on same nickel membrane with a 400μm 2-flute end mill cutter having a cutting edge radius of ~3μm at 20,000 and 100,000 rpm, respectively.

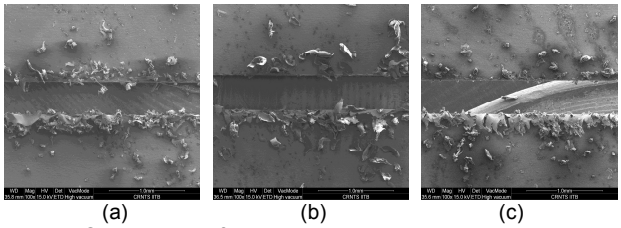

(a) (b) (c)

Fig.13. SEM images of machined micro slots in low speed milling RPM=20000 for different feed rates: (a) 0.1 μm/tooth/rev; (b) 2 μm/tooth/rev; (c) 4 μm/tooth/rev for 400μm tool diameter

While machining with large cutter diameter, the effects appear to be similar to the small cutter diameter with ploughing phenomenon in low feeds and cutting at higher feeds. It has been observed that the formation of fine powder during the ploughing at low feeds with large cutter diameter is significantly reduced. The burr formation occurs as shown in Fig.13 (a). The formation of the burrs in case of large tool diameter is quite similar to conventional micromilling at high feeds as shown in Figs. 13 (b) and (c). As seen for 100 μm tool, if the rotational speed is increased the process becomes extremely stable and very good quality slots are obtained as shown in Figs. 14 (a) through (c).

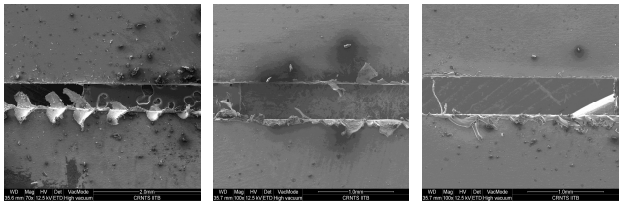

(a) (b) (c)

Fig.14. SEM images of machined micro slots in high speed milling RPM=100000 for different feed rates: (a) 0.1 μm/tooth/rev; (b) 2 μm/tooth/rev; (c) 4 μm/tooth/rev for 400μm tool diameter

At higher feed/tooth, the burr formation is negligible in case of high speed milling with a large tool diameter as shown in Fig. 14(c). The highest feed/tooth of 4 μm yields almost burr-free high quality slot. Note that this behavior is contrary to what is observed in micromilling of thick workpieces wherein the exit burrs are known to be a function of uncut chip thickness [14].

The average burr height was determined for two different tool diameter by using white light interferometry, Fig.15 shows the average burr height of 17 μm and 11.3 μm for 100 μm and 400 μm tool, respectively, for

micromilling of 20 μm thin Ni membrane. Fig. 16 shows the WLI image of 400 μm slot cut on 200μm thick Ni workpiece. The average burr height is around 2.62μm-9.5um

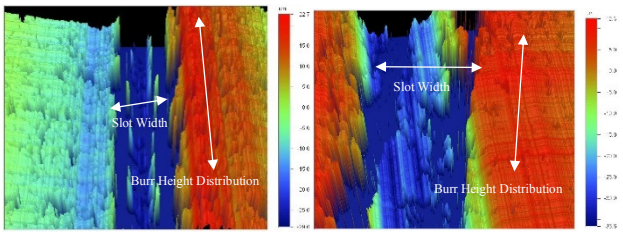

(a) (b)

Fig.15. WLI images of (a) 100μm and (b) 400μm end mill cutter on 20μm thin Ni workpiece

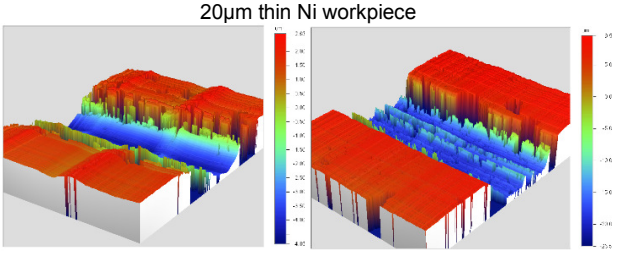

(a) (b)

Fig.16. WLI images on (a) 20000 RPM and (b) 100000μm RPM on 200μm thick Ni workpiece using 400μm end mill cutter

3.2. Effect of spindle speed, feed rate and tool diameter on the dimensional accuracy

Figures 17 and 18 show the slot width variation of machined slots throughout the length (10mm) of slot for a given rotational speed and tool diameter on 20μm thin Ni membrane. The dimensional accuracies increase as the feed increases both in low speed milling and high speed milling. The low rpm micromachining appears to be tearing dominated. It can be seen in Fig. 17(a) that the slot widths are much larger (up to 3 times larger) than the cutter diameter at low feeds. Even in high speed milling, at low feeds (see Fig. 17(b)) ploughing induced tearing occurs instead of smooth cutting and the slot widths are significantly higher than the cutter diameter (up to 2.6 times). The slot widths of the machined micro slots at low feed (0.1μm/flute) are 41%higher than that of high feeds (3 and 4μm/flute) at 100,000 rpm for 100 μm tool diameter.

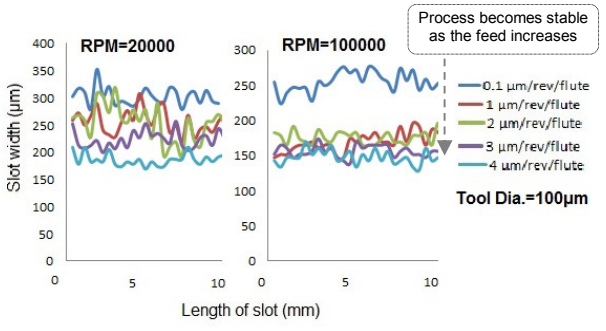

(a) (b)

Fig.17. Variation of the slot width of micro slot for different feeds in: (a) low speed micromilling; (b) high speed micromilling for 100μm end mill cutter on 20μm thin Ni workpiece

Unlike thick workpiece micromilling, where the process becomes unstable at high chip loads due to increased cutting forces, vibrations and tool wear, the ultra-thin membrane machining becomes relatively stable at high chip-loads.

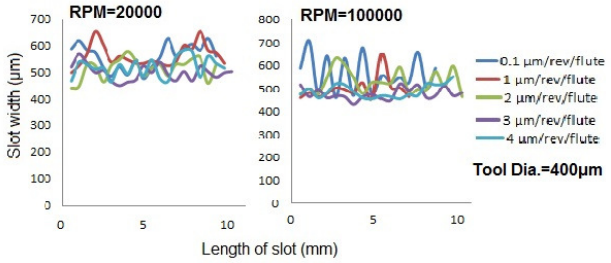

(a) (b)

Fig. 18. Variation of the slot width of micro slot for different feeds in (a) low speed micromilling and high speed micromilling for 400μm tool on 20μm thin Ni workpiece

Fig.18 shows the variation of the slot width for 400μm. The tool diameter has significant effect on the dimensional accuracy and the dependence of the slot width on the feed rate is not as pronounced as smaller tool diameter. However, the variation in the slot width across the slot length reduces as the chip-load increases as observed in both cases of smaller and larger tool diameter. Fig. 19 shows the slot width variation for 400μm tool on 200 μm thick Ni workpiece in low speed and high speed micro milling. Following the same trend as that of thin workpiece, the process becomes stable (dimensional accuracies) as the feed increases. The process becomes stable till the chip load of 3μm/flute and then gets slightly unstable opposite to the thin workpiece. This is typically what happens while machining a thick workpiece when on increasing the feed rate much higher than the cutting edge radius of the tool, the process becomes unstable lead to the higher burrs formation and tool wear. The stability regions for both thin and thick workpieces are a function of their flexural rigidity which significantly affects the cutting mechanism.

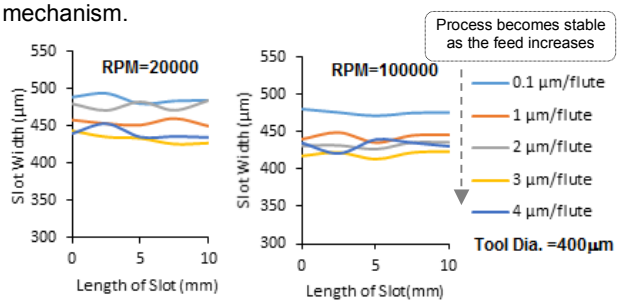

Fig. 19. Variation of the slot width of micro slot for different feeds in (a) low speed micromilling and high speed micromilling for 400μm tool on 200μm thin Ni workpiece

Fig. 20 shows the average values of the measured slot width though out the length of slots and their variation for a large spectrum of feed rates and RPM. It can be observed that a combination of high feed/tooth and high rotation speed yields the best geometric accuracy. The smallest possible geometric errors are 50% and 19% for 100 and 400 μm tool diameter, respectively.

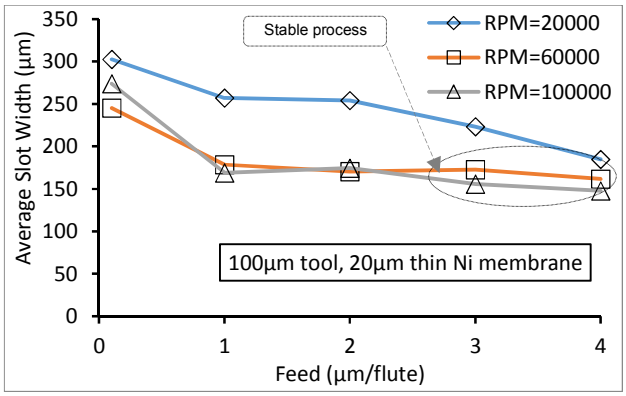

(a)

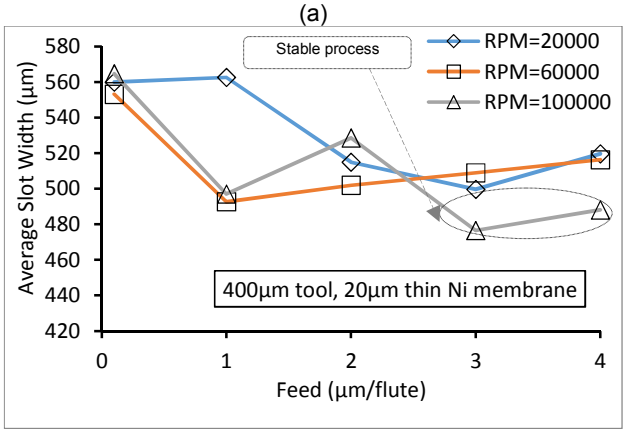

(b)

Fig.20. Average slot width of 10 mm long micro slot machined on 20 µm thick Nickel membrane for: (a) 100 µm end mill cutter; (b) 400 µm end mill cutter

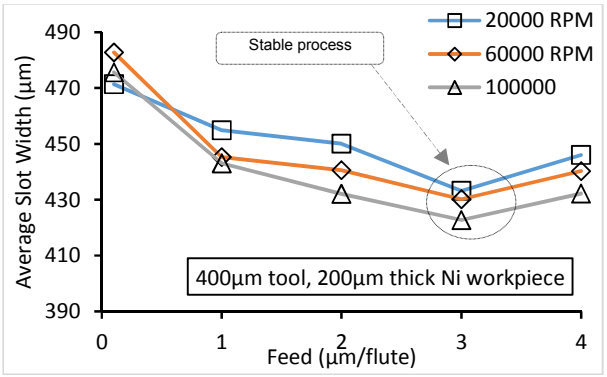

Fig. 21. Average slot width of 10mm long micro slot machined on 200 µm thick Ni workpiece for 400 µm end mill cutter

Fig. 21 shows the average slot width for thick Ni workpiece. Unlike thin worpiece, the process first gets stable till the cutting edge radius of the tool and then becomes slightly worse. This might be possible because of sudden transition due to edge radius effect may affect the forces. The minimum error for the slot width is achieved at feed of 3 µm/flute. But the higher cutting speed are always favorable for the process in both cases. The minimum error of 7% is achieved at 100000 RPM in terms of geometrical characteristics (slot width).

4. Conclusions

The following key conclusion can be drawn from the current work:

- The cutting coefficients are bigger and edge coefficients are smaller than those of the conventional end mills, which can be possible because of round edges making the effective rake angle smaller or even negative.
- The maximum prediction error of 20% is observed with the mechanistic force model.
- As the spindle speed and feed increases the process becomes stable for membrane machining. The average slot width for 100 µm and 400 µm tool was found to be approximately 150µm and 470 µm with corresponding dimensional inaccuracy of 50% and 19% respectively both at the high spindle speeds and feeds for 20µm thin Ni membrane
- The minimum average slot width for 200 µm thick Ni workpiece was found to be 428µm using 400µm end mill cutter with the geometric inaccuracies of 7%.

References

[1] Ng, S., and Wang, Z., 2008, "Hot Roller Embossing for Microfluidics: Process and Challenges," Microsyst. Technol., 15(8), pp. 1149–1156.

[2] Ishizawa, N., Idei, K., Kimura, T., Noda, D., and Hattori, T., 2008, "Resin Micromachining by Roller Hot Embossing," Microsyst. Technol., 14(9–11), pp. 1381–1388.

[3] Hupert, M. L., Guy, W. J., Llopis, S. D., Shadpour, H., Rani, S., Nikitopoulos, D. E., and Soper, S. A., 2007, "Evaluation of Micromilled Metal Mold Masters for the Replication of Microchip Electrophoresis Devices," Microfluid. Nanofluid., 3(1), pp. 1–11.

[4] Sean Ashman, *A review of manufacturing processes for microchannel heat exchanger fabrication*, "Proceedings of ICNMM2006 Fourth International Conference on Nanochannels, Microchannels and Minichannels June 19-21, 2006, Limerick, Ireland"

[5] Hupert, M. L., Guy, W. J., Llopis, S. D., Situma, C., Rani, S., Nikitopoulos, D. E., and Soper, S. A., 2006, "High-Precision Micromilling for Low-Cost Fabrication of Metal Mold Masters," Proceedings of the Microfluidics, BioMEMS, and Medical Microsystems IV, San Jose, CA, SPIE, p. 61120B.

[6] SaptajiKushendarsyah, Orthogonal Microcutting of Thin Workpieces,Journal of Manufacturing Science and Engineering | Volume 135

[7] Biermann, D. and Baschin, A., *Influence of cutting edge geometry and cutting edge radius on the stability of micromilling processes*. Production Engineering, 2009. 3(4-5): p. 375-380, ISSN: 1433-3015.

[8] W.Y. Bao, I.N. Tansel, Modeling micro-end-milling operations. Part I: Analy- tical cutting force model, International Journal of Machine Tools and Manufacture 40 (2000) 2155–2173.

[9] N. Ikawa, S. Shimada, H. Tanaka, Minimum thickness of cut in micromachin- ing, Nanotechnology 3 (1) (1992) 6–9.

[10] S.N. Melkote, W.J. Endres, The importance of including the size effect when modeling slot milling, Transaction of ASME Journal of Manufacturing Science and Engineering 120 (1998) 68–75.

[11] M.P. Vogler, S.G. Kapoor, R.E. DeVor, On the modeling and analysis of machining performance in micro end milling, part II: cutting force prediction, ASME Journal of Manufacturing Science and Engineering 126 (4) (2004) 695–705.

[12] Mohammad Malekian, SimonS.Park ,, MartinB.G.Jun 'Modeling of dynamic micromilling cutting forces' International Journal of Machine Tools & Manufacture 49 (2009) 586–598

[13] Y.V. Srinivasa, M.S. Shunmugam, 'Mechanistic model for prediction of cutting forces in micro end-milling and experimental comparison' International Journal of Machine Tools & Manufacture 67 (2013) 18–27

[14] Vivek Bajpai, et al. Burr formation and surface quality in high speed micromilling of titanium alloy (ti6ai4v), Proceedings of the ASME 2013 international manufacturing science and engineering conference, MSEC 2013, MSEC 2013-12